Brain death and organ donation

Hoeksma, Dane

CHAPTER 6

MnTMPyP, a selective superoxide dismutase mimetic, reduces oxidative stress in kidneys of brain-dead rats

D Hoeksma
PJ Ottens
S Veldhuis
H van Goor
H Leuvenink

In preparation

ABSTRACT

Introduction

Delayed graft function (DGF) is a common complication in renal transplant recipients receiving kidneys from brain-dead donors. DGF is associated with acute rejection, chronic allograft failure, and decreased renal function. Brain death (BD)-related oxidative stress, measured as malondialdehyde (MDA) levels, correlates well with DGF. Therefore, we aimed to decrease renal oxidative stress in brain-dead rats through pre-treatment with MnTMPyP, a superoxide dismutase mimetic.

Methods

BD induction was performed on 32 mechanically ventilated male Fisher rats by inflating a 4.0 F Fogarty catheter in the epidural space. Rats were observed for 4 h And maintained hemodynamically stable through the administration of colloids and norepinephrine. Plasma, urine, and kidney tissue were collected for analysis. MnTMPyP (5.0 mg/kg) or saline vehicle was administered intraperitoneally 30 min prior to BD induction.

Results

BD resulted in increased levels of renal superoxide, renal and serum MDA levels, renal oxidized glutathione, and renal HO-1 expression compared to sham values. These changes were all attenuated by MnTMPyP pre-treatment. BD also led to increased plasma creatinine levels, urinary NAG activity, renal leukocyte influx, and renal IL-6, TNF-α, and E-selectin gene expression which were not reduced by MnTMPyP pre-treatment.

Conclusion

MnTMPyP pre-treatment of brain-dead rats leads to decreased oxidative stress in kidneys of brain dead rats. Amongst others, BD-related MDA levels were decreased which correlate with DGF. Therefore, MnTMPyP treatment of brain-dead donors could lead to decreased incidence of DGF and thereby better renal transplantation outcomes.

INTRODUCTION

Delayed graft function (DGF) is a serious complication in renal transplant recipients[1-3]. DGF is associated with acute rejection, chronic allograft failure, and decreased renal function[4,5]. Kidneys from brain-dead donors, the most frequently transplanted kidneys, show DGF rates of 15-30%[5,6]. These findings are not attributed to human leukocyte antigen (HLA) mismatches, longer cold ischemia times, or donor age[7]. Rather, brain death (BD) elicits detrimental effects in the donor which affect future donor grafts[8-10].

BD leads to increased serum levels of the lipid peroxidation marker malondialdehyde (MDA) which indicates oxidative membrane damage[9,11]. MDA levels in the preservation solution of kidneys retrieved from brain-dead donors correlate well with DGF in renal transplant recipients[11]. Moreover, donor serum MDA levels correlate with acute rejection and immediate and long-term renal allograft function. In expanded criteria donors (ECD), MDA levels in machine perfusion solution also correlate with DGF[12].

Endogenous antioxidants regulate the levels of reactive oxygen species (ROS) accurately[13]. However, pathological conditions can increase oxidant production and overwhelm antioxidant defenses. Increased oxidant production results from dysfunctional oxidant producing enzymes such as xanthine oxidase, NADPH oxidase, nitric oxide synthase, and mitochondrial electron transport chain complexes[14]. Superoxide is the primary formed oxidant from these enzymes and increased levels are reported after BD[15,16]. Excessive ROS production can subsequently impair antioxidant enzymes[17]. A disbalance in production and metabolism of ROS leads to oxidative damage of cellular components such as proteins, nucleic acids, and lipid membranes[18].

Manganese (III) tetrakis(1-methyl-4-pyridyl) porphyrin (MnTMPyP) is a cell permeable superoxide dismutase mimetic with beneficial renal effects in models of sepsis and ischemia-reperfusion (I-R) injury[19-21]. In these models, the decrease in superoxide levels results in improved renal function and decreased inflammation. Furthermore, by decreasing superoxide levels, MnTMPyP prevents peroxynitrite formation, a highly potent oxidant[22].

With the present study, we aimed to decrease renal oxidative stress and thereby serum MDA levels which correlate with DGF, acute rejection and post-transplant renal function in renal transplant recipients. To achieve this goal, we pre-treated brain-dead rats with the superoxide scavenger MnTMPyP.

MATERIALS AND METHODS

Animal BD model

Male adult Fisher F344 rats (250-300 g) were anesthetized using isoflurane and subsequently intubated. The left femoral artery and vein were cannulated for blood pressure monitoring and administration of plasma expanders or norepinephrine. A no. 4 Fogarty catheter (Edwards Lifesciences Co., Irvine, CA, USA) was placed in the epidural space through a frontolateral burr-hole in the skull. The catheter was inflated (16 µl/min) with saline using a syringe pump (Terufusion, Termo Co., Tokyo, Japan). Inflation at this speed leads to increased levels of renal oxidative stress compared to faster inflation[15]. The increase in intracranial pressure (ICP) leads to BD after approximately 30 min. Inflation of the balloon was stopped when the mean arterial pressure (MAP) reached 80 mmHg due to the catecholamine storm characteristic for BD. BD was confirmed by the absence of corneal reflexes. Anesthesia was stopped after BD confirmation and the animals remained ventilated with O_2/air. MAP was kept between 80-120 mmHg by using 10% hydroxyethyl

starch (HAES) (Fresenius Kabi AG, Bad Homburg, Germany) and noradrenaline (NA) if necessary. After 4 h of BD, blood was collected through the abdominal artery after which the organs were flushed with saline. Centrifuged blood samples and urine from the bladder were snap frozen. Kidneys were harvested and sections stored in formalin as well as snap frozen. Rats were randomly divided between groups as listed below. Sham-operated rats were anesthetized, received a burr-hole, and were ventilated for half an hour under anesthesia before sacrifice. MnTMPyP (5.0 mg/kg) or saline vehicle was administered intraperitoneally, 30 min before the start of the operation.

Rats were randomly assigned to one of the following experimental groups:

Group 1: sham-operated rats receiving vehicle (N=8)
Group 2: sham-operated rats receiving MnTMPyP (N=7)
Group 3: brain-dead rats receiving vehicle (N=7)
Group 4: brain-dead rats receiving MnTMPyP (N=7)

Biochemical determinations

Plasma levels of creatinine and sodium were determined at the clinical chemistry lab of the University Medical Center Groningen per standard procedures.

Determination of superoxide production with dihydroethidium staining

Superoxide production was determined as described before 15. Four µm cryosections were mounted on slides and washed with Dulbecco's phosphate-buffered saline (DPBS). Sections were incubated with 10 µM dihydroethidium (Sigma, St. Louis, MO, USA) dissolved in DPBS at 37°C in dark conditions for 30 min. Subsequently, sections were washed twice with DPBS and scanned for superoxide with a Leica inverted fluorescence microscope equipped with rhodamine filter settings. Images were acquired at 40X magnification and analyzed using NCBI ImageJ.

Determination of lipid peroxidation with thiobarbituric acid reactive substances

Lipid peroxidation levels were determined as described before 15. MDA was measured fluorescently after binding to thiobarbituric acid. Twenty µL of kidney tissue homogenates or plasma were mixed with 2% SDS and 5mM butylated hydroxytoluene followed by 400 µL 0.1 N HCL, 50 µL 10% phosphotungstic acid and 200 µL 0.7% TBA. The mixture was incubated for 1 hr at 97°C. Eight-hundred µL 1-butanol was added to the samples and centrifuged at 960 g. Two-hundred µL of the 1-butanol supernatant was fluorescently measured at 480 nm excitation and 590 nm emission wavelengths. Samples were corrected for amount of protein and expressed as µmol/g protein.

Glutathione measurements

Glutathione measurements were conducted as described before[23]. Tissue was lysed in cell lysis buffer composed of 253 M HEPES, 5 mM $MgCl_2$, 5mM Ethylenediaminetetraacetic acid (EDTA), 2mM phenylmethylsulfonyl fluoride (PMSF) and 10 ng/µl pepstatin and leupeptin. The buffer was adjusted to a final pH of 7.5. Cell suspensions were centrifuged and the supernatant was analyzed. To measure total glutathione, 20 µl of the supernatant was added to buffer A (125 mM $NaH_2PO_4.H_20$ and 6.3 mM NaEDTA adjusted to pH 7.5 with NaOH) to a total volume of 100 µl in a transparent flat bottom 96-well plate. Next, 20 µl of 6 mM 5-5'-dithiobis-2-nitrobenzoate, 42 µl of 0.3 mM nicotinamide adenine dinucleotide phosphate (NADPH), all dissolved in buffer A, were added to the wells. Finally, 38 µl of glutathione reductase, dissolved to an enzyme activity of 5 units/ml in buffer A, was added

to the wells. The absorbance was measured at 430 nm for 15 min at 30 °C. The linear part of the kinetic curve was used for the rate estimation and compared with a standard curve of oxidized glutathione (GSSG). Samples were corrected for total amount of protein and expressed as µmol/g protein. To measure GSSG, 1-methyl-2-vinyl pyridinium triflate was added at a concentration of 3 mM to the supernatant to block reduced glutathione (GSH). GSH content was calculated by subtracting GSSG from the total glutathione values.

Heme oxygenase-1 immunohistological staining

Renal heme oxygenase-1 (HO-1) staining was performed on paraffin sections (4 µm). Sections were de-waxed, rehydrated, and subjected to heat-induced antigen retrieval by microwave heating in 1 mM EDTA (pH=8.0). Endogenous peroxidase was blocked with 0.03% H_2O_2 in PBS for 30 min. Incubation of the primary antibody lasted for 60 min at room temperature. Binding of the antibody was detected by incubation with appropriate peroxidase-labelled secondary and tertiary antibodies (Dakopatts, Glostrup, Denmark) for 30 min at room temperature. Antibody dilutions were made in PBS supplemented with 1% bovine serum albumin (BSA) and 1% normal rat serum. Peroxidase activity was visualized using 3,3'-diaminobenzidine tetrahydrochloride. Sections were counterstained with hematoxylin. Negative antibody controls were performed in which the primary antibody was omitted. HO-1 quantification was achieved by using the positive field algorithm provided by Aperio ImageScope version 11.1.2.760. Results are expressed as the proportion of the total number of positive pixels and the total number of pixels.

Granuolocyte immunological staining

Five-micrometer renal sections were fixed in acetone and stained with mouse monoclonal anti-rat granulocyte antibody (IQ products, Groningen, the Netherlands) which was dissolved in PBS (pH 7.4) supplemented with 1% bovine serum albumin (BSA). The peroxidase-labeled second antibody (rabbit anti-mouse) was diluted in 1% BSA/PBS containing 5% normal rat serum. Aminoethylcarbazole was used to visualize peroxidase activity. Sections were counterstained with hematoxylin. Control sections were incubated with omission of the primary antibody. For each tissue section, positive cells per field were counted by a blinded researcher in ten microscopic fields of the tissue at 20× magnification. Results were presented as number of positive cells per field.

RNA isolation and quantitative polymerase chain reaction

Quantitive polymerase chain reaction (qPCR) was performed as described before[9]. The SV Total RNA isolation kit (Promega, Leiden, the Netherlands) was used to isolate total RNA from rat kidneys per manufacturer's protocol. RT-PCR reactions were performed to verify samples for the absence of genomic DNA contamination, in which the addition of reverse transcriptase was omitted, using GADPH primers. cDNA synthesis was performed from 1 µg total RNA using T11VN oligo's and M-MLV reverse transcriptase, per supplier's protocol (Invitrogen, Breda, The Netherlands). The ABI Prism 7900-HT Sequence Detection System (Applied Biosystems, Foster city, CA, USA) was used for amplification and detection using emission from SYBR green. All assays were performed in triplicate. PCR cycles consisted of an initial activation step at 50°C for 2 min and a hot start at 95°C for 10 min, after which the cycles consisted of 40 cycles of 95°C for 15 s and 60°C for 60 s. Specificity of qPCR products was assessed with a dissociation curve at the end of the amplification program and by gel electrophoresis. Gene expression was normalized with the mean of β-actin mRNA content and calculated relative to controls using the relative standard curve method. Results were expressed as $2^{-}\Delta ct$ (CT threshold cycle). Amplification primers were designed with Primer Express software and validated in a six-step 2-fold dilution series. The primer sequences and product sizes are given in table 1.

Table 1. qPCR primer sequences of the genes b-actin and IL-6.

Gene	Primer Sequences	Bp
b-actin	5′-GGAAATCGTGCGTGACATTAAA-3′ 5′-GCGGCAGTGGCCATCTC-3′	74
IL-6	5′-CCAACTTCCAATGCTCTCCTAATG-3′ 5′- TTCAAGTGCTTTCAAGAGTTGGAT-3′	89
TNF- α	5′-GGCTGCCTTGGTTCAGATGT-3′ 5′-CAGGTGGGAGCAACCTACAGTT-3′	79
E-selectin	5′-GTCTGCGATGCTGCCTACTTG-3′ 5′-CTGCCACAGAAAGTGCCACTAG-3′	73

NAG injury biomarker

To estimate tubular damage, N-acetyl-β-D-glucosaminidase (NAG) activity in urine was measured using a method based on enzymatic hydrolysis of p-Nitrophenyl N-acetyl-β-D-glucosaminidase to p-Nitrophenyl and N-acetyl-β-D-glucosaminidase. Enzymatic activity was expressed as the amount of enzyme required to release 1 µmol of product per minute. NAG levels were corrected for urine creatinine levels and expressed as U/mmol UCr.

Statistical analyses

Data were analyzed using GraphPad Prism 5.04 (GraphPad, San Diego, USA). Groups were compared using the Kruskall-Wallis test with Dunns post-hoc correction. $P < 0.05$ was considered statistically significant. All data are expressed as the mean ± SD (standard deviation)

RESULTS

Hemodynamic changes and donor management during BD

BD induction showed the characteristic drop and subsequent increase in blood pressure over a mean of 30.5 min as was described before[15]. All animals were kept at a mean arterial pressure higher than 80 mmHg during the experiment. No differences were observed in blood pressure profiles between groups (Figure 1). No statistical differences were observed in amount of HAES and NA administration between groups (Table 2).

Table 2. Total Noradrenaline (1 mg/ml) and HAES infusion requirements per group.

	BD + saline	BD + MnTMPyP	P value
Noradrenaline (ml)	0.31 ± 0.1	0.28 ± 0.3	0.54
HAES (ml)	3.5 ± 0.4	4.1 ± 2.5	0.28

* indicates a significant difference between MnTMPyP- and saline-treated brain-dead rats.

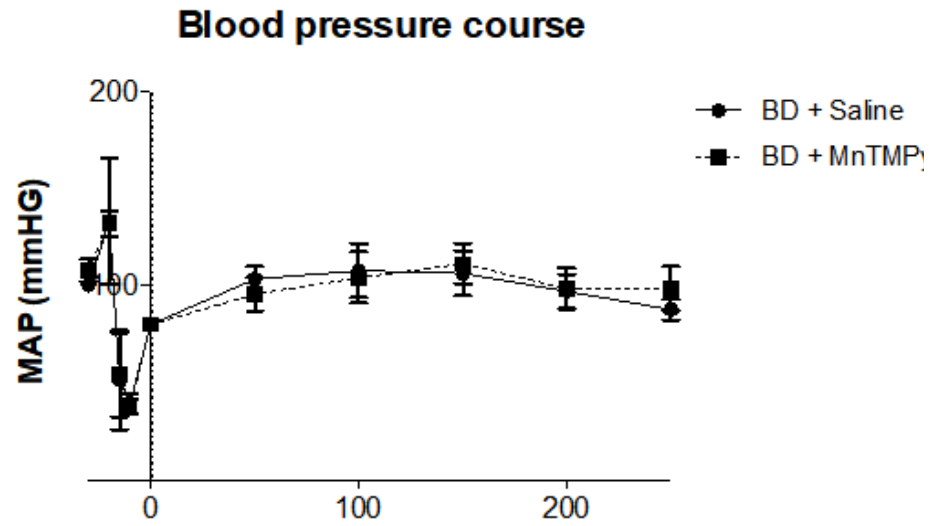

Figure 1. Blood pressure course during the induction and brain-dead phase. The induction phase showed a characteristic drop in blood pressure. No differences were observed in blood pressure levels between saline and MnTMPyP-treated brain-dead groups.

Superoxide production with dihydroethidium staining

BD led to significantly increased levels of superoxide compared to sham values ($p < 0.05$, respectively, Figure 2). Superoxide levels were significantly reduced in brain-dead rats pre-treated with MnTMPyP ($p < 0.01$).

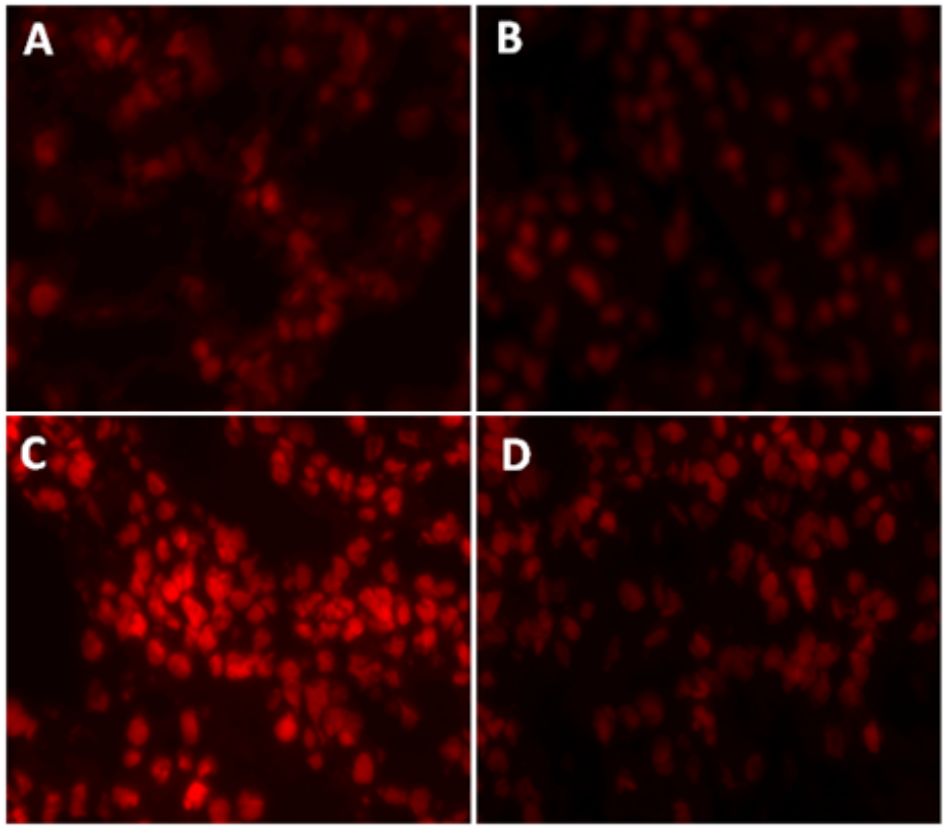

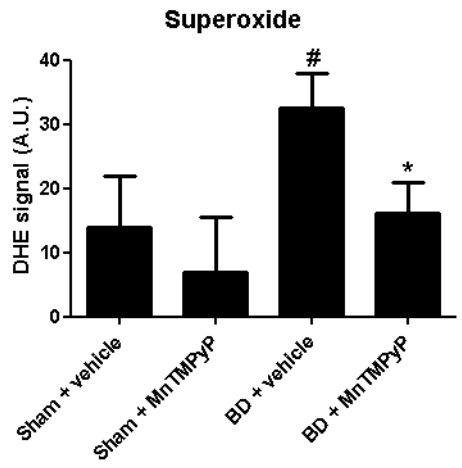

Figure 2. DHE staining for renal superoxide in sham-operated and brain-dead rats. A, sham + vehicle. B, sham + MnTMPyP. C, brain death + vehicle, and D, brain death + MnTMPyP. BD led to increased superoxide production compared to sham-operated rats which was markedly decreased by MnTMPyP pre-treatment. * indicates $p < 0.05$ compared to vehicle-treated brain-dead rats. # indicates $p < 0.05$ compared to sham-operated rats. 40X magnification

Lipid peroxidation

Renal and serum MDA levels were increased significantly by BD compared to sham values ($p < 0.01$, Figure 3). Both renal and serum MDA levels were significantly decreased by MnTMPyP pre-treatment ($p < 0.01$ and $p < 0.05$, respectively).

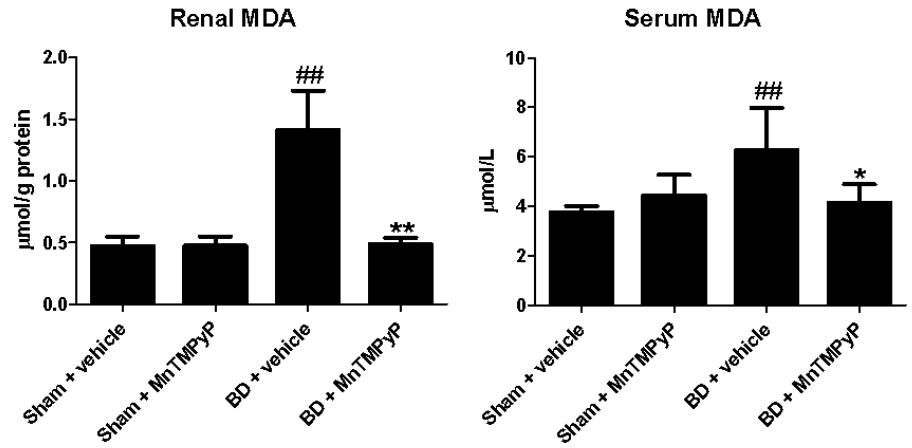

Figure 3. Renal and serum levels of lipid peroxidation in sham-operated and brain-dead rats. BD resulted in significant increases of renal and serum MDA levels which were attenuated by MnTMPyP pre-treatment. * indicates $p < 0.05$ compared to vehicle-treated brain-dead rats. ## indicates $p < 0.01$ compared to sham-operated rats

GSH, GSSG, GSH + GSSG, and the GSSG:GSH ratio

BD did not lead to decreased GSH levels compared to sham-operated rats. However, brain-dead rats pre-treated with MnTMPyP resulted in significantly increased GSH levels compared to saline-treated brain-dead rats ($p < 0.01$, figure 4). BD did lead to significantly increased levels of GSSG which were significantly attenuated by MnTMPyP pre-treatment ($p < 0.01$). Also, BD led to an increased GSSG:GSH ratio which was significantly attenuated by MnTMPyP pre-treatment ($p < 0.05$).

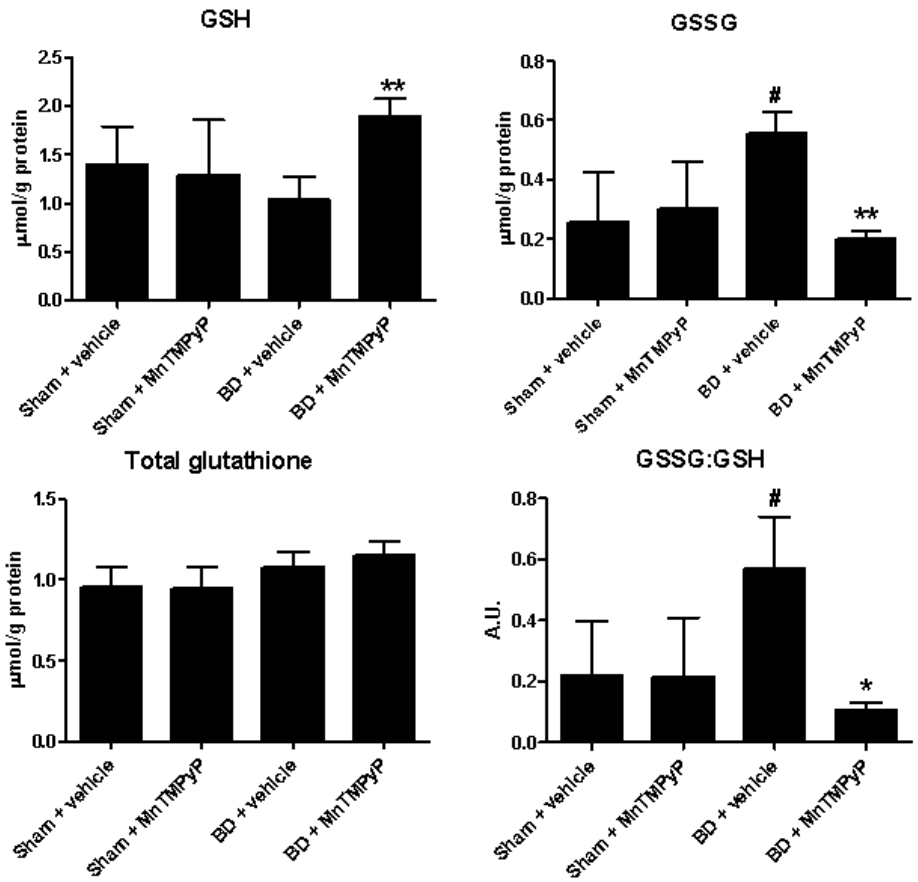

Figure 4. Renal levels of reduced glutathione (GSH), oxidized glutathione (GSSG), total glutathione (GSH+GSSG) and the ratio of oxidized to reduced glutathione GSSG:GSH) in sham-operated and brain-dead rats. MnTMPyP pre-treatment of brain-dead rats resulted in significantly increased GSH levels compared to saline-treated brain dead rats. BD resulted in significantly increased GSSG levels and GSSG:GSH ratio which were reduced significantly by MnTMPyP pre-treatment. * and ** indicate $p < 0.05$ and 0.01, respectively, compared to vehicle-treated brain-dead rats. # indicates $p < 0.05$ compared to sham-operated rats.

HO-1 protein expression

BD led to a significant increase in renal HO-1 expression compared to sham-operated rats ($p < 0.01$, figure 5). This increase was significantly attenuated in rats pre-treated with MnTMPyP ($p < 0.05$).

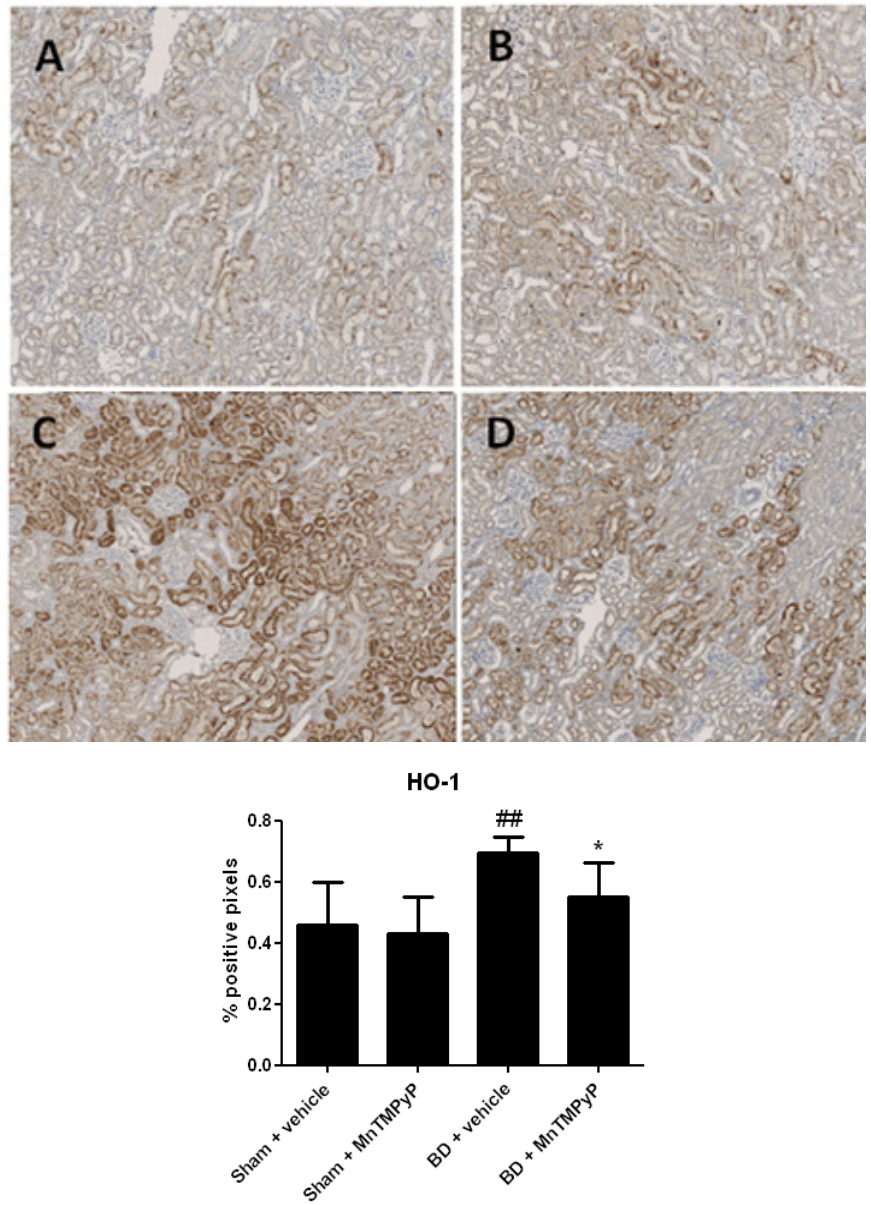

Figure 5. Renal expression of the cytoprotective protein heme oxygenase-1 (HO-1) in sham-operated and brain-dead rats. BD resulted in significantly increased HO-1 expression compared to sham-operated rats which was markedly decreased by MnTMPyP pre-treatment. ## indicates $p < 0.01$ compared to sham-operated rats.
* indicates $p < 0.05$ compared to saline-treated brain-dead rats. 100x magnification.

Granulocyte protein expression

BD led to a significant increase in renal cortical granulocyte expression compared to sham-operated rats ($p < 0.01$, figure 6). This increase was not decreased by MnTMPyP pre-treatment.

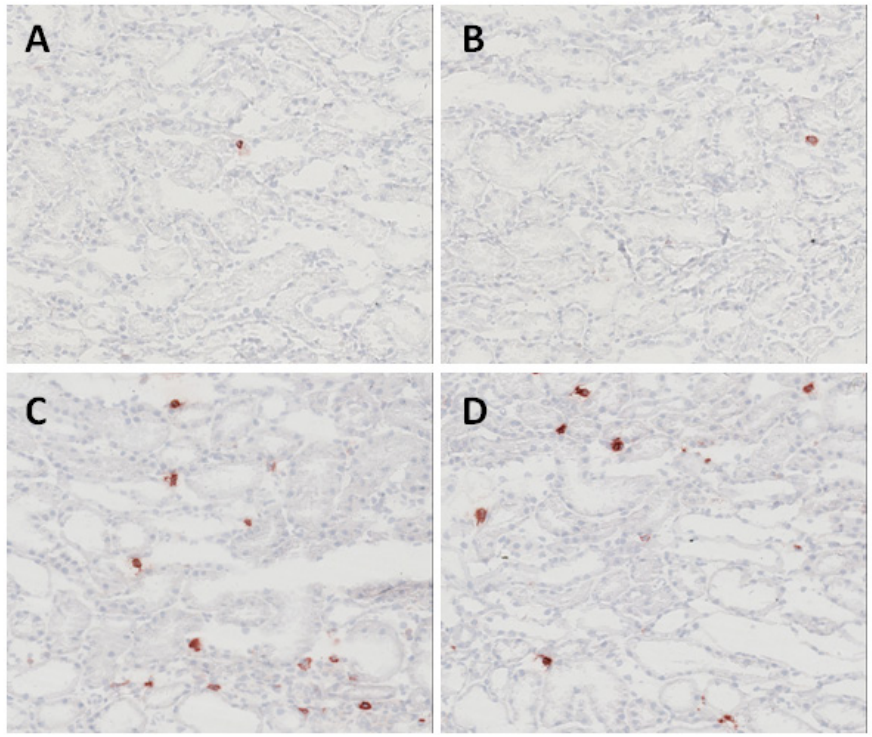

Figure 6. Renal influx of polymorphonuclear (PMN) leukocytes in sham-operated and brain-dead rats. BD resulted in significantly increased PMN influx compared to sham-operated rats which was not attenuated by MnTMPyP treatment. ## indicates $p < 0.01$ compared to sham-operated rats. 20x magnification.

Renal gene expression levels

Renal mRNA levels of interleukin-6 (IL-6), TNF-α, and E-selectin 6 were significantly increased in brain-dead rats compared to sham-operated animals (Figure 7) which was not attenuated by MnTMPyP pre-treatment.

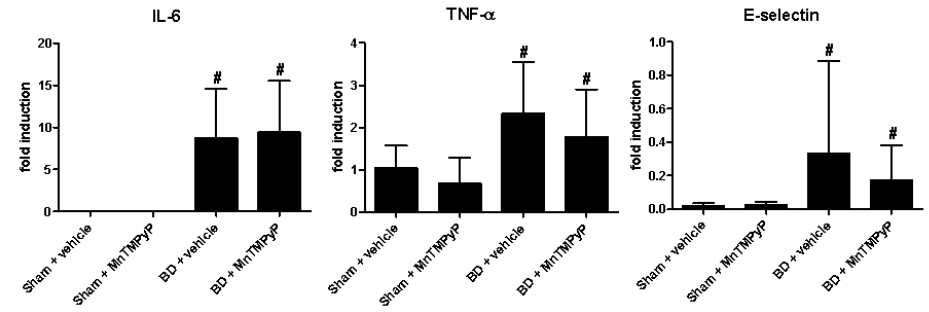

Figure 7. Renal expression of the pro-inflammatory genes IL-6, TNF-α, and E-selectin in sham-operated and brain-dead rats. BD led to significant increase in renal IL-6, TNF- α, and E-selectin expression. MnTMPyP pre-treatment did not result in decreased expression of these genes. # indicates $p < 0.05$ compared to sham-operated rats. compared to sham-operated rats. 20x magnification.

Biochemical determinations

BD resulted in increased plasma creatinine levels and decreased creatinine clearance compared to sham-operated rats (table 3). Also, BD resulted in increased fractional sodium excretion. These effects were not affected by MnTMPyP pre-treatment.

Table 3. Biochemical parameters

	Sham + saline	Sham + MnTMPyP	BD + saline	BD + MnTMPyP
Crs, µmol/L	34.86 ± 7.20	34.29 ± 6.45	96.00 ± 22.62 #	102.71 ± 27.80
CrC, ml/min	0.38 ± 0.04	0.37 ± 0.03	0.24 ± 0.08 #	0.28 ± 0.09
FeNa, %	1.2± 0.1	1.1 ± 0.1	1.7 ± 0.3 #	1.5 ± 0.3
Urinary NAG, U/mmol UCr	0.04 ± 0.03	0.03 ± 0.27	0.10 ± 0.36 ##	0.08 ± 0.13

Variables measured 4 hrs after BD or immediately after sham procedure
significant at $p < 0.05$ compared to sham-operated rats
significant at $p < 0.05$ compared to sham-operated rats

Urinary NAG activity

After 4 hours of BD, urinary NAG activity was significantly increased compared to sham-operated rats ($p < 0.01$, table 3). The increase in NAG activity was not decreased by MnTMPyP pre-treatment.

DISCUSSION

As a proof of concept, we showed that pre-treatment of brain-dead rats with MnTMPyP, a superoxide scavenger, resulted in decreased renal oxidative stress. MnTMPyP pre-treatment led to the reduction of oxidative stress markers, amongst others renal and serum MDA levels, which are a marker of lipid peroxidation and indicate oxidative membrane damage. Brain death (BD)-related lipid peroxidation correlates well with DGF, acute rejection, and post-transplant renal function[11]. Therefore, MnTMPyP treatment of brain-dead-donors could lead to decreased incidence of above mentioned processes and thereby improved transplantation outcomes (Figure 8).

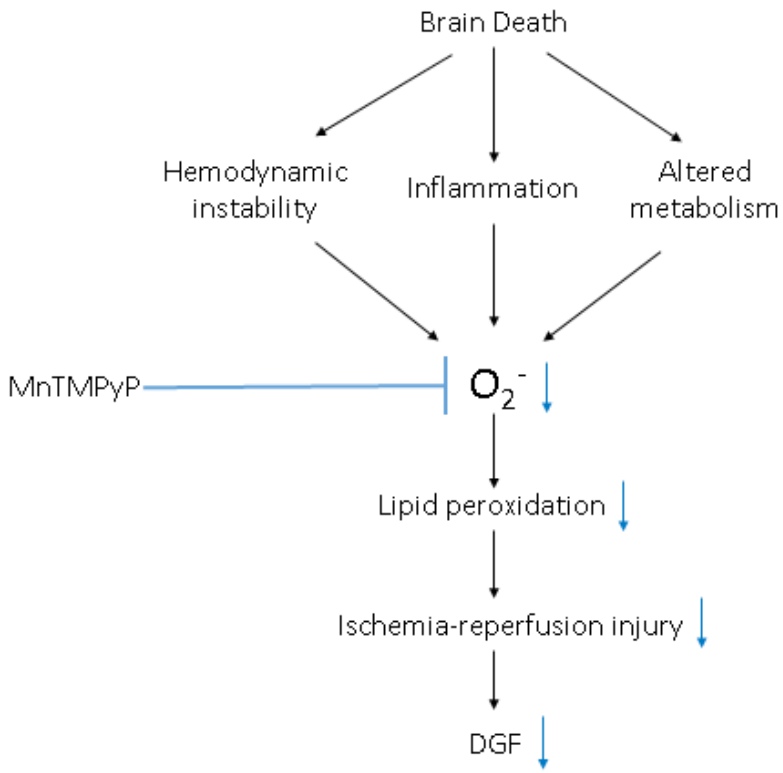

Figure 8. Proposed mechanism of decreased lipid peroxidation in brain-dead donors by MnTMPyP treatment and subsequent decreased risk of IR-injury and DGF (simplified). Brain death leads to increased superoxide production through hemodynamic instability, inflammation, and altered metabolism. MnTMPyP treatment decreases superoxide levels and thereby lipid peroxidation. Lipid peroxidation levels in the brain-dead donor correlate positively with DGF in renal transplant recipients. Therefore, we postulate that decreased lipid peroxidation in the brain-dead donor leads to less susceptibility to IR-injury and DGF.

Lipid peroxidation leads to membrane dysfunction and subsequent cell toxicity[24-26]. It has been shown previously that lipid peroxidation related to aging leads to increased I-R injury upon reperfusion and results in damaged mitochondria[27]. Recently, post-transplant mitochondrial damage was shown to cause a metabolic deficit resulting in the development of DGF[28]. Since BD-related lipid peroxidation is associated with DGF, we

postulate that the observed lipid peroxidation in brain-dead donors renders cells more susceptible to I-R injury which leads to increased mitochondrial damage after reperfusion and thereby leads to increased risk of DGF.

The compound MnTMPyP was very effective in our model as renal and plasma MDA levels were reduced to sham values. However, in our study, as a proof of concept, MnTMPyP was administered before BD induction and not during BD. In future studies, the effect of MnTMPyP administration during BD should be evaluated to assess the clinical feasibility of this compound. Since MDA levels only become evident after 2 hours of BD, we hypothesize that the administration of MnTMPyP after BD confirmation will lead to the same effects as observed with pre-treatment[8,9,15].

Glutathione is regarded as a major anti-oxidative molecule because of its high cellular concentrations and the central role it fulfills in redox reactions[29-31]. Glutathione can serve as a cofactor for anti-oxidative enzymes but can also react directly with oxidants such as superoxide[32]. The glutathione disulfide (GSSG)/glutathione (GSH) ratio is a traditional marker for reflecting the level of cellular oxidative stress[33]. In our study, BD led to an increased GSSG/GSH ratio which was decreased by MnTMPyP treatment. Interestingly, increased GSSG levels did not coincide with decreased GSH levels which indicates GSH levels are replenished during BD. In a previous study, we showed that renal GSH levels decreased after 2 hours of BD but returned to reference levels after 4 hours[15]. Renal glutathione synthesis is totally dependent on the uptake of glutathione conjugates from the circulation[34,35]. Therefore, the unchanged renal GSH levels could be the result of the increased plasma glutathione levels we observed during BD in the aforementioned study[15]. Increased plasma glutathione is likely the result of glutathione release into the circulation through hepatic apoptosis which has been shown previously[36]. Since renal GSH levels do not remain decreased during BD, increasing GSH levels in brain-dead donors could be futile. Indeed, it has been shown that the administration of n-acetylcysteine to brain-dead donors does not lead to decreased incidence of DGF in renal transplant recipients[37].

HO-1 may be among the most critical cytoprotective mechanisms that are activated during times of cellular stress such as inflammation, ischemia, hypoxia, hyperoxia, hyperthermia, or radiation[38]. HO-1 has found to be increasingly expressed during BD which reflects the need of cytoprotection under these conditions[39-41]. In this light, it is understandable that transplanting kidneys from brain-dead donors in which HO-1 was induced, led to better graft survival[42,43]. However, in our study, renal HO-1 expression was significantly reduced by MnTMPyP treatment indicating a decrease of the trigger for HO-1 expression and a cardinal role of superoxide in the development of BD-related renal cellular stress. Transplanting kidneys from brain-dead donors treated with MnTMPyP could therefore lead to similar beneficial results compared to studies in which HO-1 was induced.

Through its antioxidant properties, MnTMPyP has shown to improve markers of inflammation, damage, and renal function in several models[19-21,44]. In rat models of renal I-R injury, MnTMPyP treatment leads to decreased damage markers, renal levels of inflammatory markers, infiltrating granulocytes and plasma creatinine levels[19]. However, MnTMPyP pre-treatment did not lead to the above-mentioned effects in the present study. The explanation for this observation could be that in I-R injury, anoxia is the primary insult which results in damage, an inflammatory process, and decreased renal function, whereas in BD, the relative ischemia is not severe enough to cause similar effects. Moreover, in BD, inflammatory processes are likely also initiated through other mechanisms than solely ischemia, such as the dying brain.

In conclusion, MnTMPyP pre-treatment of brain-dead rats leads to decreased renal oxidative stress during BD. Amongst others, the oxidative membrane damage marker MDA, which correlates with DGF, acute rejection, and post-transplant renal function in renal transplant recipients, was reduced by MnTMPyP pre-treatment. Therefore, treatment of brain-dead donors with MnTMPyP could lead to decreased incidences of above mentioned processes and thereby improved transplantation outcomes.

ACKNOWLEDGMENTS

We would like to thank Jacco Zwaagstra and Janneke Wiersema-buist for their excellent technical assistance in the laboratory.

REFERENCES

1. OPTN/SRTR 2011 Annual Data Report. Available at: Http://Srtr.transplant.hrsa.gov/annual_reports/2011/flash/01_kidney/index.html#/1/zoomed. .
2. Siedlecki A, Irish W, Brennan DC. Delayed graft function in the kidney transplant. Am J Transplant. 2011;11(11):2279-2296.
3. Peeters P, Vanholder R. Therapeutic interventions favorably influencing delayed and slow graft function in kidney transplantation: Mission impossible? Transplantation. 2008;85(7 Suppl):S31-7.
4. Wu WK, Famure O, Li Y, Kim SJ. Delayed graft function and the risk of acute rejection in the modern era of kidney transplantation. Kidney Int. 2015;88(4):851-858.
5. Perico N, Cattaneo D, Sayegh MH, Remuzzi G. Delayed graft function in kidney transplantation. Lancet. 2004;364(9447):1814-1827.
6. Moers C, Kornmann NS, Leuvenink HG, Ploeg RJ. The influence of deceased donor age and old-for-old allocation on kidney transplant outcome. Transplantation. 2009;88(4):542-552.
7. Terasaki PI, Cecka JM, Gjertson DW, Takemoto S. High survival rates of kidney transplants from spousal and living unrelated donors. N Engl J Med. 1995;333(6):333-336.
8. Morariu AM, Schuurs TA, Leuvenink HG, van Oeveren W, Rakhorst G, Ploeg RJ. Early events in kidney donation: Progression of endothelial activation, oxidative stress and tubular injury after brain death. Am J Transplant. 2008;8(5):933-941.
9. Schuurs TA, Morariu AM, Ottens PJ, et al. Time-dependent changes in donor brain death related processes. Am J Transplant. 2006;6(12):2903-2911.
10. Novitzky D, Cooper DK, Morrell D, Isaacs S. Change from aerobic to anaerobic metabolism after brain death, and reversal following triiodothyronine therapy. Transplantation. 1988;45(1):32-36.
11. Kosieradzki M, Kuczynska J, Piwowarska J, et al. Prognostic significance of free radicals: Mediated injury occurring in the kidney donor. Transplantation. 2003;75(8):1221-1227.
12. Nagelschmidt M, Minor T, Gallinat A, et al. Lipid peroxidation products in machine perfusion of older donor kidneys. J Surg Res. 2013;180(2):337-342.
13. Wiernsperger NF. Oxidative stress: The special case of diabetes. Biofactors. 2003;19(1-2):11-18.
14. Valko M, Leibfritz D, Moncol J, Cronin MT, Mazur M, Telser J. Free radicals and antioxidants in normal physiological functions and human disease. Int J Biochem Cell Biol. 2007;39(1):44-84.
15. Hoeksma D, Rebolledo RA, Hottenrott CM, et al. Inadequate anti-oxidative responses in kidneys of brain-dead rats. Transplantation. 2016.
16. Murphy MP. How mitochondria produce reactive oxygen species. Biochem J. 2009;417(1):1-13.
17. Pigeolet E, Corbisier P, Houbion A, et al. Glutathione peroxidase, superoxide dismutase, and catalase inactivation by peroxides and oxygen derived free radicals. Mech Ageing Dev. 1990;51(3):283-297.
18. Galley HF. Bench-to-bedside review: Targeting antioxidants to mitochondria in sepsis. Crit Care. 2010;14(4):230.
19. Liang HL, Hilton G, Mortensen J, Regner K, Johnson CP, Nilakantan V. MnTMPyP, a cell-permeant SOD mimetic, reduces oxidative stress and apoptosis following renal ischemia-reperfusion. Am J Physiol Renal Physiol. 2009;296(2):F266-76.
20. Seija M, Baccino C, Nin N, et al. Role of peroxynitrite in sepsis-induced acute kidney injury in an experimental model of sepsis in rats. Shock. 2012;38(4):403-410.

21. Wang Z, Holthoff JH, Seely KA, et al. Development of oxidative stress in the peritubular capillary microenvironment mediates sepsis-induced renal microcirculatory failure and acute kidney injury. Am J Pathol. 2012;180(2):505-516.
22. Nin N, El-Assar M, Sanchez C, et al. Vascular dysfunction in sepsis: Effects of the peroxynitrite decomposition catalyst MnTMPyP. Shock. 2011;36(2):156-161.
23. Griffith OW. Determination of glutathione and glutathione disulfide using glutathione reductase and 2-vinylpyridine. Anal Biochem. 1980;106(1):207-212.
24. Yajima D, Motani H, Hayakawa M, Sato Y, Sato K, Iwase H. The relationship between cell membrane damage and lipid peroxidation under the condition of hypoxia-reoxygenation: Analysis of the mechanism using antioxidants and electron transport inhibitors. Cell Biochem Funct. 2009;27(6):338-343.
25. Dix TA, Aikens J. Mechanisms and biological relevance of lipid peroxidation initiation. Chem Res Toxicol. 1993;6(1):2-18.
26. Wong-Ekkabut J, Xu Z, Triampo W, Tang IM, Tieleman DP, Monticelli L. Effect of lipid peroxidation on the properties of lipid bilayers: A molecular dynamics study. Biophys J. 2007;93(12):4225-4236.
27. Lucas DT, Szweda LI. Cardiac reperfusion injury: Aging, lipid peroxidation, and mitochondrial dysfunction. Proc Natl Acad Sci U S A. 1998;95(2):510-514.
28. Wijermars LG, Schaapherder AF, de Vries DK, et al. Defective postreperfusion metabolic recovery directly associates with incident delayed graft function. Kidney Int. 2016;90(1):181-191.
29. Franco R, Schoneveld OJ, Pappa A, Panayiotidis MI. The central role of glutathione in the pathophysiology of human diseases. Arch Physiol Biochem. 2007;113(4-5):234-258.
30. Franco R, Cidlowski JA. Apoptosis and glutathione: Beyond an antioxidant. Cell Death Differ. 2009;16(10):1303-1314.
31. Forman HJ, Zhang H, Rinna A. Glutathione: Overview of its protective roles, measurement, and biosynthesis. Mol Aspects Med. 2009;30(1-2):1-12.
32. Winterbourn CC, Metodiewa D. The reaction of superoxide with reduced glutathione. Arch Biochem Biophys. 1994;314(2):284-290.
33. Harris C, Hansen JM. Oxidative stress, thiols, and redox profiles. Methods Mol Biol. 2012;889:325-346.
34. Ormstad K, Jones DP, Orrenius S. Characteristics of glutathione biosynthesis by freshly isolated rat kidney cells. J Biol Chem. 1980;255(1):175-181.
35. Rankin BB, Wells W, Curthoys NP. Rat renal peritubular transport and metabolism of plasma [35S] glutathione. Am J Physiol. 1985;249(2 Pt 2):F198-204.
36. Rebolledo RA, Hoeksma D, Hottenrott CM, et al. Slow induction of brain death leads to decreased renal function and increased hepatic apoptosis in rats. J Transl Med. 2016;14(1):141-016-0890-0.
37. Orban JC, Quintard H, Cassuto E, Jambou P, Samat-Long C, Ichai C. Effect of N-acetylcysteine pretreatment of deceased organ donors on renal allograft function: A randomized controlled trial. Transplantation. 2015;99(4):746-753.
38. Choi AM, Alam J. Heme oxygenase-1: Function, regulation, and implication of a novel stress-inducible protein in oxidant-induced lung injury. Am J Respir Cell Mol Biol. 1996;15(1):9-19.
39. Nijboer WN, Schuurs TA, van der Hoeven JA, et al. Effect of brain death on gene expression and tissue activation in human donor kidneys. Transplantation. 2004;78(7):978-986.
40. Bos EM, Schuurs TA, Kraan M, et al. Renal expression of heat shock proteins after brain death induction in rats. Transplant Proc. 2005;37(1):359-360.
41. van Dullemen LF, Bos EM, Schuurs TA, et al. Brain death induces renal expression of heme oxygenase-1 and heat shock protein 70. J Transl Med. 2013;11:22-5876-11-22.
42. Fontana J, Yard B, Stamellou E, et al. Dopamine treatment of brain-dead fisher rats improves renal histology but not early renal function in lewis recipients after prolonged static cold storage. Transplant Proc. 2014;46(10):3319-3325.
43. Kotsch K, Francuski M, Pascher A, et al. Improved long-term graft survival after HO-1 induction in brain-dead donors. Am J Transplant. 2006;6(3):477-486.
44. Pathak E, MacMillan-Crow LA, Mayeux PR. Role of mitochondrial oxidants in an in vitro model of sepsis-induced renal injury. J Pharmacol Exp Ther. 2012;340(1):192-201.